




## Correlated Coulomb-Volkov approach and its application to the angular distributions of two-photon double ionization of helium

Arnaud Denabe , M. Silenou Mengoue ,\* and M. G. Kwato Njock 

Centre for Atomic, Molecular Physics and Quantum Optics, Faculty of Science, *University of Douala*, P.O. Box 8580, Douala, Cameroon



(Received 4 March 2024; accepted 31 May 2024; published 17 June 2024)

We investigate the double-ionization process of helium in brief and intense laser fields of 10, 16, and 40 optical cycles, linearly polarized with an intensity of  $5 \times 10^{12} \text{ W cm}^{-2}$ . We calculate the total two-photon double-ionization cross section for photon energies ranging from 39.5 to 54 eV and the triple-differential cross sections at a photon energy of 42 eV, using the correlated Coulomb-Volkov approach, which takes into account the interaction of the laser field with each electron (Volkov phase) and interactions of Coulombian nature between electrons and between electrons and the nucleus. The proposed wave function has the advantage of being much less time consuming due to the fact that it does not require a numerical propagation of the wave packet. The results of our calculations obtained for the nonsequential double photoionization are compared with previously reported data and good agreement is found with approaches using projections onto uncorrelated continuum states. This indicates that the disagreements that remain between some theoretical models for the process studied cannot simply be attributed to the electronic correlation in the continuum states.

DOI: [10.1103/PhysRevA.109.062810](https://doi.org/10.1103/PhysRevA.109.062810)

### I. INTRODUCTION

Understanding and characterizing the correlation between two active electrons is the basis for understanding the dynamics of a multielectron systems in intense laser fields. Double photon ionization (DPI) is the most fundamental multiphoton process which provides a new opportunity for exploring the electron correlation effects. As the simplest and the most fundamental multielectron system, helium atoms have showed great advantages in the exploration of electron correlation dynamics. The most detailed description of this process, also known as the  $(\gamma, 2e)$  reaction, can be obtained in the form of the fully resolved triply differential cross section (TDCS), which gives the probability of detecting the two photoelectrons with fully determined kinematics.

In the long-pulse-duration limit, DPI processes are classified into two types, namely, sequential and nonsequential processes. The sequential mechanism dominates when one photon ionizes the ground-state He into  $\text{He}^+$  (step 1) and then the other photon ionizes  $\text{He}^+$  to  $\text{He}^{2+}$  (step 2). This sequential process is possible and dominant if the photon energy is higher than the ionization potential of  $\text{He}^+$ . In contrast, the nonsequential or direct double-ionization process dominates when the photon energy is lower than the second ionization potential but still higher than half of the sum of the first- and second-ionization potentials. The second electron could

not be liberated independently by absorbing one photon and thus requires the reassignment of excess energy through the electron correlation.

More precisely, since the ground-state energies of He and  $\text{He}^+$  are  $-79.0$  and  $-54.4$  eV, the first- and second-ionization potentials will be 24.6 and 54.4 eV, respectively. If the photon energy is higher than 54.4 eV, DPI of helium can be treated as a sequential process, in which the first electron can be ionized by absorbing one photon and the second electron can be ionized by absorbing another photon. If the photon energy is lower than 54.4 eV but higher than 39.5 eV, the energy of one photon is no longer high enough to induce the ionization of  $\text{He}^+$ , which means the sequential picture is inapplicable; however, the total energy of two photons is high enough to induce the double ionization of helium. That is the case in this work, where the photon energy is chosen to be 42 eV, which is higher than 39.5 eV but lower than 54.4 eV; our study falls then into the nonsequential regime.

Concerning the specific aspect of the nonsequential mechanism involving the electron correlation, it should be noted that intense theoretical activities have been developed to describe the atomic structure of helium, in particular through the development of well-formulated wave functions for the ground state [1–6]. For instance, one well-understood process is the one-photon double ionization (1PDPI) of helium, for which theoretical predication and experimental measurements have achieved excellent agreement on the total and differential double-ionization cross sections [7–9]. However, a more complex process, such as the two-photon double ionization of helium, has continued to attract great interest.

Given the intensities and lengths of the laser pulses involved, the numerical approaches used to tackle this problem are all essentially attempting to solve the time-dependent Schrödinger equation, beginning with a well-defined initial

\*Contact author: [smengoue@yahoo.fr](mailto:smengoue@yahoo.fr)

Published by the American Physical Society under the terms of the [Creative Commons Attribution 4.0 International license](https://creativecommons.org/licenses/by/4.0/). Further distribution of this work must maintain attribution to the author(s) and the published article's title, journal citation, and DOI.

state before the laser strikes and then propagating this state in the presence of the laser field by one of a number of numerical approaches. Once the laser is switched off, various probabilities and, in some cases, generalized cross sections can be extracted. Among them, in terms of the most recent works, Zhang *et al.* [10] employed spherical coordinates and the close-coupling scheme to treat the angular coordinates analytically. The Coulomb repulsion between two electrons was treated by solving a Poisson equation. The final state was made by projecting the wave function onto the product of two Coulomb waves after propagating for a long time until reaching the supposed asymptotic region. Simonsen *et al.* [11] employed spherical coordinates and the time-dependent wave function expanded in a basis of  $B$  splines. The double continuum is approximated by the product of one-electron Coulomb  $\text{He}^+(r)$  and with  $Z = 2$  projected onto different angular channels of the final wave function at  $t = \tau$ .

However, two-photon double ionization (2PDI) remains a wide open subject because of disagreements between the different theoretical results and even between the two existing experimental results [12–15]. In particular, there has been speculation that the representation of the double continuum might be responsible for the existing differences. Nevertheless, even for methods that take correlation into account in the final states, the cross sections obtained still disagree, and a systematic change in the results due to the improved treatment of electronic correlation has not yet been observed [16].

Compared to the total cross section, the present knowledge of the differential cross sections of the 2PDI of He also remains limited [17]. It is well known that the fully resolved TDCS contains the most detailed information on the two-electron breakup process. In this case, we are aware of, for example, potential convergence problems due to TDCS sensitivity to the choice of angular momentum, especially for kinematic situations where the cross section is small, e.g., at  $\theta_1 = 90^\circ$ . Kheifets *et al.* [17–19] obtained results for this situation by using the convergent close-coupling approach to describe the final two-electron continuum state. The results in their two works differ significantly, both from each other and from those presented by authors such as Guan *et al.* [20], Zhang *et al.* [10], Hu *et al.* [21], and Feist *et al.* [16]. In addition, experimental angular distribution results are not yet available.

Considering the issue thus important, our present work aims to know to what extent a correlated Coulomb-Volkov approach (CCVA) could be situated in this new field of study. Thus, from the expression of the transition amplitude established in our CCVA, we propose to deduce the probability density and use it in the angular distributions when the two ejected outgoing electrons share equally the photon's excess energy. This approach, which takes into account the electron correlation in the initial and final states, has the advantage of being a much less time consuming method due to the fact that it does not require numerical propagation of the wave packet. Such a method was employed in [22], where the authors used uncorrelated initial and final states and then improved them progressively. This increased their workload in terms of analytical developments and numerical calculations as a consequence. We have extended the approach to describe the final state of our system, composed of the product of two

Volkov phases (which takes into account the interaction of the laser field with each electron) and a function expanded into the Sturmian basis (which describes the interaction of the nucleus with each electron and the electron-electron correlation). For the initial state, aware of the important role electronic correlation plays, we used a fully correlated wave function with all Coulomb interactions taken into account as described and developed in details in [23,24].

The paper is organized as follows. In Sec. II we briefly describe our theoretical method for the numerical solution of the full-dimensional time-dependent Schrödinger equation (TDSE) for the two electrons of a helium atom interacting with brief and intense laser pulses. In Sec. III we present our results. The total two-photon double-ionization cross section is presented, followed by the results of the triple-differential cross sections. Our results are then compared with those available in some previous works in order to demonstrate the accuracy of our numerical scheme. We provide a brief summary in Sec. IV. Atomic units are used throughout.

## II. THEORETICAL CALCULATIONS

In order to investigate the dynamics of helium in three dimensions, for the two-electron quantum systems interacting with brief and intense laser pulses, we consider the time-dependent Schrödinger equation

$$i \frac{\partial}{\partial t} |\Psi(\mathbf{r}_1, \mathbf{r}_2, t)\rangle = [H_0 + H_{\text{int}}(t)] |\Psi(\mathbf{r}_1, \mathbf{r}_2, t)\rangle, \quad (1)$$

where  $H_0$  is the Hamiltonian of the nonperturbative system, given by

$$H_0 = -\frac{1}{2} \nabla_1^2 - \frac{1}{2} \nabla_2^2 - \frac{Z}{r_1} - \frac{Z}{r_2} + \frac{1}{r_{12}}, \quad (2)$$

and  $\mathbf{r}_1$  and  $\mathbf{r}_2$  are the position vectors of electrons 1 and 2, respectively, with  $r_{12} = |\mathbf{r}_1 - \mathbf{r}_2|$  the interelectronic distance. Here  $Z = 2$  is the charge of the infinitely massive nucleus, the position of which coincides with the origin of the laboratory system.

In the following,  $H_{\text{int}}(t)$  represents the interaction between the laser field and the atomic system, written in the length gauge as

$$H_{\text{int}}(t) = -(\mathbf{r}_1 + \mathbf{r}_2) \cdot \mathbf{E}(t), \quad (3)$$

where  $\mathbf{E}(t)$  is the time-dependent laser field. Studies of the gauge invariance of the strong-field-approximation model including the Volkov phase can be found in [25–27]. In this work, the laser pulse is assumed to be linearly polarized and the two electrons are assumed to be initially in their ground state. The linearly polarized laser pulse is modeled with a sine-squared carrier envelope and given by

$$\mathbf{E}(t) = E_0 \sin(\omega t + \varphi) \sin^2\left(\frac{\pi t}{\tau}\right) \mathbf{e}_z, \quad t \in [0, \tau], \quad (4)$$

where  $E_0$  denotes the peak strength of the electric field. The pulse duration is  $\tau = 2\pi n_c / \omega$ , where  $n_c$  is the number of optical cycles and  $\omega$  the laser frequency (referred to as the photon energy). The pulse is made symmetric with respect to  $t = \tau/2$  by setting the phase  $\varphi = (\omega t - \pi)/2$ . We stress that the phase  $\varphi$  matters little when many oscillations are

performed during the pulse. Here  $A(t)$ , the time-dependent classical vector potential describing the laser pulse, is linked to  $\mathbf{E}(t)$  by

$$\mathbf{E}(t) = -\frac{\partial \mathbf{A}(t)}{\partial t}. \quad (5)$$

To evaluate the physical observables and extract the physical information from the ionization process, we employ a correlated double continuum wave function. Suppose the two electrons are emitted into the continuum with momenta  $\mathbf{k}_i$  ( $i = 1, 2$ ), with energies denoted by  $E_1$  and  $E_2$  ( $E = E_1 + E_2$ ). The transition amplitude for such a process deduced from Eq. (1) is

$$T_{fi}^- = -i \int dt \int d\mathbf{r}_1 d\mathbf{r}_2 \Psi_f^{-*}(\mathbf{r}_1, \mathbf{r}_2; t)(\mathbf{r}_1 + \mathbf{r}_2) \times \mathbf{E}(t) \Psi_i(\mathbf{r}_1, \mathbf{r}_2; t), \quad (6)$$

where  $\Psi_f^- *(\mathbf{r}_1, \mathbf{r}_2; t)$  is the correlated Coulomb-Volkov double continuum wave function and  $\Psi_i(\mathbf{r}_1, \mathbf{r}_2; t)$  our initial-state wave function detailed in [23],

$$\Psi_f^{-*}(\mathbf{r}_1, \mathbf{r}_2; t) = \psi^{-*}(\mathbf{k}_1, \mathbf{k}_2; \mathbf{r}_1, \mathbf{r}_2; t) \mathcal{L}^{-*}(\mathbf{k}_1, \mathbf{k}_2; \mathbf{r}_1, \mathbf{r}_2; t), \quad (7)$$

with  $\mathcal{L}^{-*}(\mathbf{k}_1, \mathbf{k}_2; \mathbf{r}_1, \mathbf{r}_2; t)$  the product of two Volkov phases [28] which take into account the interaction of the laser field with each electron

$$\begin{aligned} \mathcal{L}^{-*}(\mathbf{k}_1, \mathbf{k}_2; \mathbf{r}_1, \mathbf{r}_2; t) &= \exp[-i\mathbf{A}(t) \cdot \mathbf{r}_1] \exp[-i\mathbf{A}(t) \cdot \mathbf{r}_2] \\ &\times \exp\left(i\mathbf{k}_1 \int_{\tau}^t dt' \mathbf{A}(t')\right) \\ &\times \exp\left(i\mathbf{k}_2 \int_{\tau}^t dt' \mathbf{A}(t')\right). \end{aligned} \quad (8)$$

In Eq. (7),  $\psi^{-*}(\mathbf{k}_1, \mathbf{k}_2; \mathbf{r}_1, \mathbf{r}_2; t)$  is a function describing the interaction of the nucleus with each electron and which takes into account the electron-electron correlation. It could be expressed as

$$\begin{aligned} \psi^{-*}(\mathbf{k}_1, \mathbf{k}_2; \mathbf{r}_1, \mathbf{r}_2; t) \\ = \mathcal{A} \psi^{-*}(\mathbf{k}_1, \mathbf{k}_2; \mathbf{r}_1, \mathbf{r}_2) \exp(i\varepsilon_{k_1} t) \exp(i\varepsilon_{k_2} t). \end{aligned} \quad (9)$$

In addition,  $\psi^-(\mathbf{k}_1, \mathbf{k}_2; \mathbf{r}_1, \mathbf{r}_2)$  is an ingoing wave and the solution of the Schrödinger equation

$$\left(E + \frac{1}{2}\nabla_1^2 + \frac{1}{2}\nabla_2^2 + \frac{Z}{r_1} + \frac{Z}{r_2} - \frac{1}{r_{12}}\right) \psi^-(\mathbf{k}_1, \mathbf{k}_2; \mathbf{r}_1, \mathbf{r}_2) = 0. \quad (10)$$

Since both electrons are identical particles, we can introduce the new functions [29]  $\psi_i^-(\mathbf{k}_1, \mathbf{k}_2; \mathbf{r}_1, \mathbf{r}_2)$  ( $i = 1, 2$ ) such that  $\psi^- = (\psi_1^- + \psi_2^-)/\sqrt{2}$ . Taking into account the exchange symmetry of the solution of Eq. (10),  $\psi^-(\mathbf{k}_1, \mathbf{k}_2; \mathbf{r}_1, \mathbf{r}_2) = g\psi^-(\mathbf{k}_1, \mathbf{k}_2; \mathbf{r}_2, \mathbf{r}_1)$ , where  $g = (-1)^S$  with  $S = 0$  (singlet state) or  $S = 1$  (triplet state), we have  $\psi_2^-(\mathbf{k}_1, \mathbf{k}_2; \mathbf{r}_1, \mathbf{r}_2) = g\hat{P}_{12}\psi_1^-(\mathbf{k}_1, \mathbf{k}_2; \mathbf{r}_1, \mathbf{r}_2)$ , where  $\hat{P}_{12}$  is the permutation operator of particle indices 1 and 2. The helium singlet ground state is space symmetric and the spin quantum number  $S$  is conserved

in the dipole approximation. Throughout this work  $g = 1$ , so

$$\psi^-(\mathbf{k}_1, \mathbf{k}_2; \mathbf{r}_1, \mathbf{r}_2) = \frac{1}{\sqrt{2}}(1 + \hat{P}_{12})\psi_1^-(\mathbf{k}_1, \mathbf{k}_2; \mathbf{r}_1, \mathbf{r}_2). \quad (11)$$

Equation (10) can be rewritten as

$$\left(E + \frac{1}{2}\nabla_1^2 + \frac{1}{2}\nabla_2^2 + \frac{Z}{r_1} + \frac{Z}{r_2}\right) \psi_1^- = V(\mathbf{r}_1, \mathbf{r}_2) \psi_1^-, \quad (12)$$

where

$$V(\mathbf{r}_1, \mathbf{r}_2) = \frac{1}{r_{12}}. \quad (13)$$

Note that the operator on the left-hand side of Eq. (12) acts in the two independent subspaces  $\mathbf{r}_1$  and  $\mathbf{r}_2$ . Its free solution is a symmetrized product of two Coulomb wave functions  $\varphi^-(\mathbf{k}_1, \mathbf{r}_1) \times \varphi^-(\mathbf{k}_2, \mathbf{r}_2)$ . Solving Eq. (12) in its more convenient integral form leads to writing it as

$$\begin{aligned} \psi_1^-(\mathbf{k}_1, \mathbf{k}_2; \mathbf{r}_1, \mathbf{r}_2) &= \psi_0^-(\mathbf{k}_1, \mathbf{k}_2; \mathbf{r}_1, \mathbf{r}_2) \\ &+ \int d\mathbf{r}'_1 \int d\mathbf{r}'_2 G^-(\mathbf{r}_1, \mathbf{r}_2; \mathbf{r}'_1, \mathbf{r}'_2; E) \\ &\times V(\mathbf{r}'_1, \mathbf{r}'_2) \psi_1^-(\mathbf{k}_1, \mathbf{k}_2; \mathbf{r}'_1, \mathbf{r}'_2), \end{aligned} \quad (14)$$

with

$$\begin{aligned} \psi_0^-(\mathbf{k}_1, \mathbf{k}_2; \mathbf{r}_1, \mathbf{r}_2) &= \varphi^-(\mathbf{k}_1, \mathbf{r}_1) \varphi^-(\mathbf{k}_2, \mathbf{r}_2) \theta(k_1 - k_2) \\ &+ g\varphi^-(\mathbf{k}_1, \mathbf{r}_2) \varphi^-(\mathbf{k}_2, \mathbf{r}_1) \theta(k_2 - k_1), \end{aligned} \quad (15)$$

where  $\theta$  is the modified step function with  $\theta(0) = 1/2$  and  $G^-$  is the Green's function calculated in [23].

We now perform a partial wave decomposition of the function  $\psi_1^-$  and write

$$\begin{aligned} \psi_1^-(\mathbf{k}_1, \mathbf{k}_2; \mathbf{r}_1, \mathbf{r}_2) \\ = \frac{2}{\pi k_1 k_2} \sum_{LM} \sum_{\lambda l} [\psi_{\lambda l}(\mathbf{k}_1, \mathbf{k}_2; \mathbf{r}_1, \mathbf{r}_2) \Lambda_{\lambda l}^{LM}(\hat{\mathbf{k}}_1, \hat{\mathbf{k}}_2) \theta(k_1 - k_2) \\ + g\psi_{\lambda l}(\mathbf{k}_2, \mathbf{k}_1; \mathbf{r}_1, \mathbf{r}_2) \Lambda_{\lambda l}^{LM}(\hat{\mathbf{k}}_2, \hat{\mathbf{k}}_1) \theta(k_2 - k_1)], \end{aligned} \quad (16)$$

where  $L$  is the total angular momentum and  $M$  its projection on the quantization axis;  $\Lambda_{\lambda l}^{LM}(\hat{\mathbf{p}}, \hat{\mathbf{q}})$  is the bipolar harmonic. The expansion of the partial wave function  $\psi_{\lambda l}(\mathbf{r}_1, \mathbf{r}_2; \mathbf{k}_1, \mathbf{k}_2)$  in a basis of Coulomb-Sturmian functions [23,24] and bipolar harmonics gives

$$\psi_{\lambda l}(\mathbf{k}_1, \mathbf{k}_2; \mathbf{r}_1, \mathbf{r}_2) = \sum_{\lambda, l, n, v} C_{nv}^{L(l\lambda)}(E) P_{\kappa\kappa\nu n}^{LLM}(\mathbf{r}_1, \mathbf{r}_2), \quad (17)$$

where the coefficients  $C_{nv}^{L(l\lambda)}(E)$  are calculated in Ref. [29] and

$$P_{\kappa\kappa\nu n}^{LLM}(\mathbf{r}_1, \mathbf{r}_2) = \frac{S_{v\lambda}^{\kappa}(r_1) S_{nl}^{\kappa}(r_2)}{r_1 r_2} \Lambda_{\lambda l}^{LM}(\hat{\mathbf{r}}_1, \hat{\mathbf{r}}_2). \quad (18)$$

The initial wave function used in this work is expanded in the Sturmian basis as [23]

$$\Psi_i(\mathbf{r}_1, \mathbf{r}_2, t) = \sum_{LM=0} \sum_{\lambda, l} \sum_{\nu, n} \alpha_{\nu n}^{\lambda l} \psi_{\kappa\kappa}^{\lambda lLM}(t) \mathcal{A} P_{\kappa\kappa\nu n}^{\lambda lLM}(\mathbf{r}_1, \mathbf{r}_2), \quad (19)$$

where  $\mathcal{A} = (1 + \hat{P}_{12})/\sqrt{2}$ ,  $\alpha_{\nu n}^{\lambda l}$  controls the redundancies that, from the exchange of the electrons, may occur in the basis, and

$\psi_{\kappa\kappa}^{\lambda ILM}(t)$  is the time-dependent expansion coefficient given by

$$\psi_{\kappa\kappa}^{\lambda ILM}(t) = \psi_{\kappa\kappa}^{\lambda ILM} \exp(-i\varepsilon_{H_e} t). \quad (20)$$

To reduce and simplify  $\Psi_i(\mathbf{r}_1, \mathbf{r}_2, t)$  we write

$$\mathcal{B}_{\kappa\kappa\nu n}^{\lambda ILM} = \alpha_{\nu n}^{\lambda I} \psi_{\kappa\kappa}^{\lambda ILM}, \quad (21)$$

so

$$\Psi_i(\mathbf{r}_1, \mathbf{r}_2, t) = \sum_{LM=0} \sum_{\lambda, l} \sum_{\nu, n} \mathcal{B}_{\kappa\kappa\nu n}^{\lambda ILM} \exp(-i\varepsilon_{H_e} t) \mathcal{A} P_{\kappa\kappa\nu n}^{\lambda ILM}(\mathbf{r}_1, \mathbf{r}_2). \quad (22)$$

The transition amplitude then becomes

$$\begin{aligned} T_{(1s)^2}^{cv} = & -i \frac{2}{k_1 k_2} \frac{1}{\pi} \sum_{(L'M')(LM)} \sum_{(\lambda'l')(\lambda l)} \sum_{(\nu'n')(vn)} \mathcal{B}_{\kappa\kappa\nu n}^{\lambda ILM} C_{\nu'n'}^{*\lambda'l'L'M'} \int dt E(t) \exp\left(i(\varepsilon_{k_1} + \varepsilon_{k_2} - \varepsilon_{H_e})t + (\mathbf{k}_1 + \mathbf{k}_2) \int_{\tau}^t dt' \mathbf{A}(t')\right) \\ & \times \int d\mathbf{r}_1 d\mathbf{r}_2 \exp[-i\mathbf{A}(t) \cdot (\mathbf{r}_1 + \mathbf{r}_2)] (r_1 \cos \theta_1 + r_2 \cos \theta_2) \mathcal{A}' P_{\kappa'\kappa'\nu'n'}^{*\lambda'l'L'M'}(\mathbf{r}_1, \mathbf{r}_2) \mathcal{A} P_{\kappa\kappa\nu n}^{\lambda ILM}(\mathbf{r}_1, \mathbf{r}_2). \end{aligned} \quad (23)$$

From Eq. (23) we write the temporal term in the form (see the Appendix)

$$Q_{k_1 k_2}(t) = \int_0^{\tau} dt \mathbf{A}(t) E(t) \exp\left(i(\varepsilon_{k_1} + \varepsilon_{k_2} - \varepsilon_{H_e})t + (\mathbf{k}_1 + \mathbf{k}_2) \int_{\tau}^t dt' \mathbf{A}(t')\right). \quad (24)$$

The multipolar development allows us to transform the transition amplitude and apply it to either 1PDI or 2PDI using the Taylor expansion of  $\exp[i\mathbf{A}(t) \cdot \mathbf{r}]$  responsible for the transition [22,28]. Then we write radial terms for 2PDI as

$$\mathcal{R}(\mathbf{r}_1, \mathbf{r}_2) = \int d\mathbf{r}_1 d\mathbf{r}_2 \mathcal{A}' P_{\kappa'\kappa'\nu'n'}^{*\lambda'l'L'M'}(\mathbf{r}_1, \mathbf{r}_2) r_1 \cos \theta_1 (r_1 \cos \theta_1 + r_2 \cos \theta_2) \mathcal{A} P_{\kappa\kappa\nu n}^{\lambda ILM}(\mathbf{r}_1, \mathbf{r}_2). \quad (25)$$

The transition amplitude expression can be reduced to the numerically implementable form as

$$T_{(1s)^2}^{cv} = -i \frac{2}{k_1 k_2} \frac{1}{\pi} Q_{k_1 k_2}(t) \sum_{(L'M')(LM)} \sum_{(\lambda'l')(\lambda l)} \sum_{(\nu'n')(vn)} \mathcal{B}_{\kappa\kappa\nu n}^{\lambda ILM} C_{\nu'n'}^{*\lambda'l'L'M'} \mathcal{R}(\mathbf{r}_1, \mathbf{r}_2). \quad (26)$$

The density of probability is then calculated using the transition amplitude as

$$\mathcal{D}_{(1s)^2}(k_1, k_2, \Omega_1, \Omega_2) = |T_{(1s)^2}^{cv}|^2 \quad (27)$$

or as a function of ejected electrons energies as

$$\mathcal{D}_{(1s)^2}(E_1, E_2, \Omega_1, \Omega_2) = k_1 k_2 |T_{(1s)^2}^{cv}|^2. \quad (28)$$

The triply differential cross section for emitting one electron with energy  $E_1$  into the solid angle  $\Omega_1$  while the second one is emitted into  $\Omega_2$  is given by

$$\frac{d^3\sigma}{dE_1 d\Omega_1 d\Omega_2} = \left(\frac{\omega}{I_0}\right)^2 \frac{1}{T_{\text{eff},2}} \int dE_2 \mathcal{D}_{(1s)^2}(E_1, E_2, \Omega_1, \Omega_2) \quad (29)$$

where  $T_{\text{eff},2} = 35\tau/128$ .

Note that the TDCSs presented in this paper are all calculated in coplanar geometry where the electric-field vector of the linearly polarized laser field and the momentum vectors of the two escaping electrons all lie in the same plane.

### III. RESULTS AND DISCUSSION

In this section we present the results of our simulation of nonsequential 2PDI of helium by the theoretical approach described above (the CCVA). The result for the total two-photon double-ionization cross section is first presented and compared to other approaches followed by the TDCSs for different angular configurations.

The initial condition of the time-dependent Schrödinger equation is the helium ground state, obtained by partial diagonalization of the field-free Hamiltonian of helium. The calculations were performed using the initial-state wave function expanded in the Sturmian basis. Note that the efficiency of this spectral method has been confirmed by calculating the helium ground-state energy. In our expansion basis, with nonlinear parameters  $\kappa_1 = \kappa_2 = 2$  and  $l_{\text{max}} = 7$  (maximum value for the individual angular momenta), we obtained  $E_0 = -2.903\,552\,646\,632$  a.u. for the ground-state energy, which represents 99.98% of the best theoretical value reported by Drake [30]. This result validated our spectral method as an appropriate approach to evaluate the cross sections of the helium ionization processes.

The final state chosen is the correlated Coulomb-Volkov wave function to take into account the interaction of the laser field with each electron (Volkov phase) and interactions of Coulombian nature between electrons and between electrons with the nucleus (correlated Coulomb waves) as described in Sec. II. This function was also expanded in the Sturmian basis. The maximum angular momentum values are  $L_{\text{max}} = 3$  for the total angular momentum and  $l_{1,\text{max}} = l_{2,\text{max}} = 7$  for the individual angular momenta. We found, as in the previous works [10–12,16,20], that these values are sufficient to obtain converged results. We noticed just a slight negligible difference of the cross sections between  $L_{\text{max}} = 2$  and  $L_{\text{max}} = 3$ , in term of amplitudes, which means convergence has been reached with even  $L_{\text{max}} = 2$ . The convergence observed confirmed that when the total angular momentum  $L$  is conserved for the

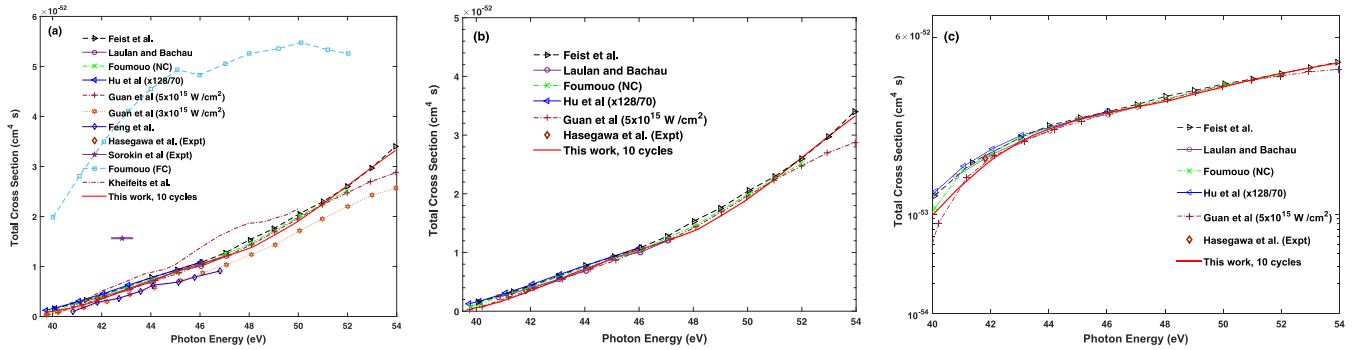


FIG. 1. Total two-photon double-ionization cross section as a function of the photon energy. The laser pulse has a sine-squared shape with a total duration of 1 fs (ten cycles). Our result shown by the red solid line, obtained with  $L_{\max} = 3$  and  $l_{1,\max} = l_{2,\max} = 7$ , is compared to the results obtained using various other theoretical approaches (see the legend) and to the experimental results of Hasegawa *et al.* [14] and Sorokin *et al.* [15]. In (a), for the results of Fomouou *et al.* [13], NC labels the results obtained by projecting onto uncorrelated Coulomb waves, while FC labels the results obtained using the  $J$ -matrix method. For the results of Guan *et al.* [20] ( $5 \times 10^{15}$  W/cm<sup>2</sup>) labels the results obtained with a peak intensity of  $5 \times 10^{15}$  W/cm<sup>2</sup> and ( $3 \times 10^{15}$  W/cm<sup>2</sup>) labels the results obtained with a peak intensity of  $3 \times 10^{15}$  W/cm<sup>2</sup>. (b) Selection of closely matching results between our approach and those presented in (a). (c) Same closely matching results as in (b), but in a log-linear scale. Note that the results of Hu *et al.* [21] were rescaled by a factor of 128/70 in order to include the correct  $T_{\text{eff}}$ .

field-free Hamiltonian (because of spherical symmetry), the expansion does not require much higher values for  $L_{\max}$  than the minimum number of photons absorbed by the system [16]. These values of angular momenta were used for the calculations of both the total cross section and the TDCS. The laser pulse applied in our calculations has a  $5 \times 10^{12}$  W/cm<sup>2</sup> peak intensity and is shaped by a sine-squared envelope function defined as

$$f(t) = \begin{cases} \sin^2(\frac{\pi t}{\tau}) & \text{for } 0 < t < \tau \\ 0 & \text{otherwise.} \end{cases} \quad (30)$$

### A. Total cross section

Figure 1 shows the total two-photon double-ionization cross section as a function of the photon energy. The photon energy varies from 39.5 eV to 54 eV. The experimental results of Hasegawa *et al.* [14] and Sorokin *et al.* [15] and the theoretical results of Feist *et al.* [16], Hu *et al.* [21] Laulan and Bachau [31], Fomouou *et al.* [13], Guan *et al.* [20], Feng and van der Hart [32], and Kheifets and Ivanov [18,33] are also presented in the figure. As shown in the legend, the red solid line is the result obtained with our approach. All results presented in Fig. 1 are obtained after ten cycles (1 fs) of laser pulse duration.

The total cross section shown in Fig. 1 is described as either explicitly or implicitly including correlation in the initial and final states. Without providing a detailed description of the various approaches used, we indicate each method employed in the calculations to which we compare ours.

Feist *et al.* [16] and Hu *et al.* [21] employed time-dependent close coupling to obtain ionizing wave packets. For the solution of the TDSE, the authors extracted transition amplitudes by projection onto uncorrelated products of Coulomb continuum functions for each electron. Laulan and Bachau [31] solved the TDSE by means of a  $B$ -spline method and an explicit Runge-Kutta propagation scheme. The dynamic calculations include electronic correlation. The final double continuum states are calculated by treating the electronic term within the zeroth- and first-order perturbation theory.

Guan *et al.* [20] employed a nonperturbative time-dependent approach based on the finite-element discrete-variable representation and an uncorrelated double continuum wave function. Feng and van der Hart [32] used correlated treatments including the  $R$ -matrix Floquet calculations in combination with  $B$ -spline basis sets. Fomouou *et al.* [13] employed a spectral method of configuration-interaction type (involving Coulomb-Sturmian functions) and an explicit Runge-Kutta time propagation to solve the TDSE and then performed projection onto the uncorrelated product of Coulomb waves, taking into account correlation by using the  $J$ -matrix method. Kheifets and Ivanov's [18,33] approach is based on the time-dependent convergent close-coupling (CCC) method, taking into account correlation in the final state to some degree.

From a general observation, most of the curves obtained with ten optical cycles have a similar shape, except the correlated calculations of Fomouou *et al.*, which we will return to later in our comparison. Most curves increase as a function of photon energy.

For photon energies between 39.5 and 46 eV, the total cross sections show an approximately linear increase with photon energy. All different theoretical approaches present practically the same shape. Above 46 eV, for those calculations with results up to 52 eV, the cross sections tend to increase a bit faster with photon energy and finally from 52 eV to 54 eV the behavior depends on the approach employed, showing a faster increase in some cases and a relatively constant tendency or slight decrease for others. In Figs. 1(b) and 1(c) the agreement of the present results with all of other presented calculations is generally within a factor of 1.2 except very near threshold. In Fig. 1(a) there is also satisfactory agreement with the results of Feng and van der Hart, though not perfect, due to the fact that these results are quite lower than ours. The correlated result reported by Kheifets and Ivanov agrees fairly well from 40 eV to 45 eV with our result and other calculations, but is much higher above 45 eV.

At a photon energy of 41.8 eV, we determine the generalized cross section for two-photon double ionization to be approximately  $3.4 \times 10^{-53}$  cm<sup>4</sup> s, which is very close

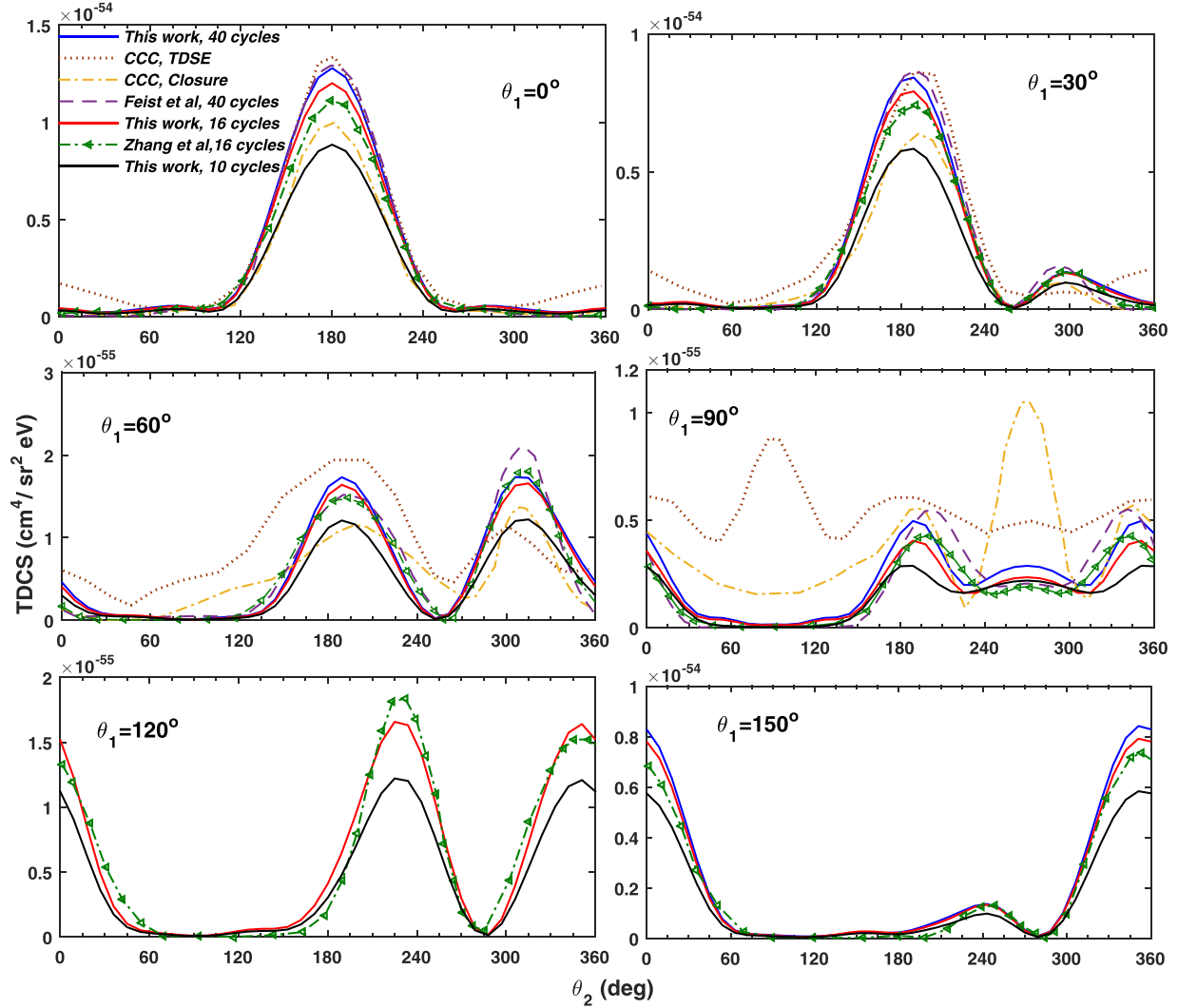


FIG. 2. Triple-differential cross section for two-photon double ionization of helium at 42 eV photon energy, for 10 cycles (black solid line), 16 cycles (red solid line), and 40 cycles (blue solid line) of a sine-squared laser pulse, at equal energy sharing and a laser peak intensity of  $5 \times 10^{12} \text{ W cm}^{-2}$ . The TDCS is given as a function of  $\theta_2$ , the angle of one of the ejected electrons. Six values of  $\theta_1$ , the angle of the other ejected electrons, are considered:  $0^\circ$ ,  $30^\circ$ ,  $60^\circ$ ,  $90^\circ$ ,  $120^\circ$ , and  $150^\circ$ . Our results are compared to the results obtained using other theoretical approaches (see the legend). They include the CCC TDSE and the CCC closure results of [18,19], the results of Feist *et al.* [16], and the results of Zhang *et al.* [10].

to the experimental cross section of  $3.63 \times 10^{-53} \text{ cm}^4 \text{ s}$  of Hasegawa *et al.* [14]. Let us finally mention that the result of Fomouou *et al.* remains higher than experimental results and all other theoretical calculations presented here. Hamido and co-workers [34] do not attribute this disagreement to the correlation that the authors accounted for. Instead, they argue that this overestimation has a highly probable cause in the reflection of the ionized wave packet and precisely of the fast electrons coming from the first channels of single ionization, at the artificial boundaries imposed by the basis functions.

### B. Triple-differential cross sections

Ten, 16, and 40 optical cycles, corresponding to total pulse durations of  $\tau = 1, 1.6$ , and  $4$ , respectively, were used to generate TDCSs curves. All plots are for the case where both

electrons share equally the excess energy of 5 eV at a photon energy of  $\omega = 42 \text{ eV}$ . Our TDCSs represented in Fig. 2 are angular distributions in the cases where electron 1 has fixed angles  $\theta_1$  of  $0^\circ$ ,  $30^\circ$ ,  $60^\circ$ ,  $90^\circ$ ,  $120^\circ$ , and  $150^\circ$  relative to the direction of polarization and plot the probability for the other electron to escape with any angular range.

In general, Fig. 2 displays various shapes of the TDCS, showing that the probability of detecting the second electron when the first one is ejected with a fixed known direction depends on the first electron ejection angle. We can also see that the extracted TDCS shows some degree of pulse-duration dependence for not long enough pulses. Calculations in all the approaches presented in Fig. 2 were done in a coplanar geometry. The TDCSs obtained with the different approaches have a similar shape, except those obtained with the CCC TDSE of Refs. [18,19]. It is useful to specify that CCC TDSE refers to the time-dependent Schrödinger equation calculation

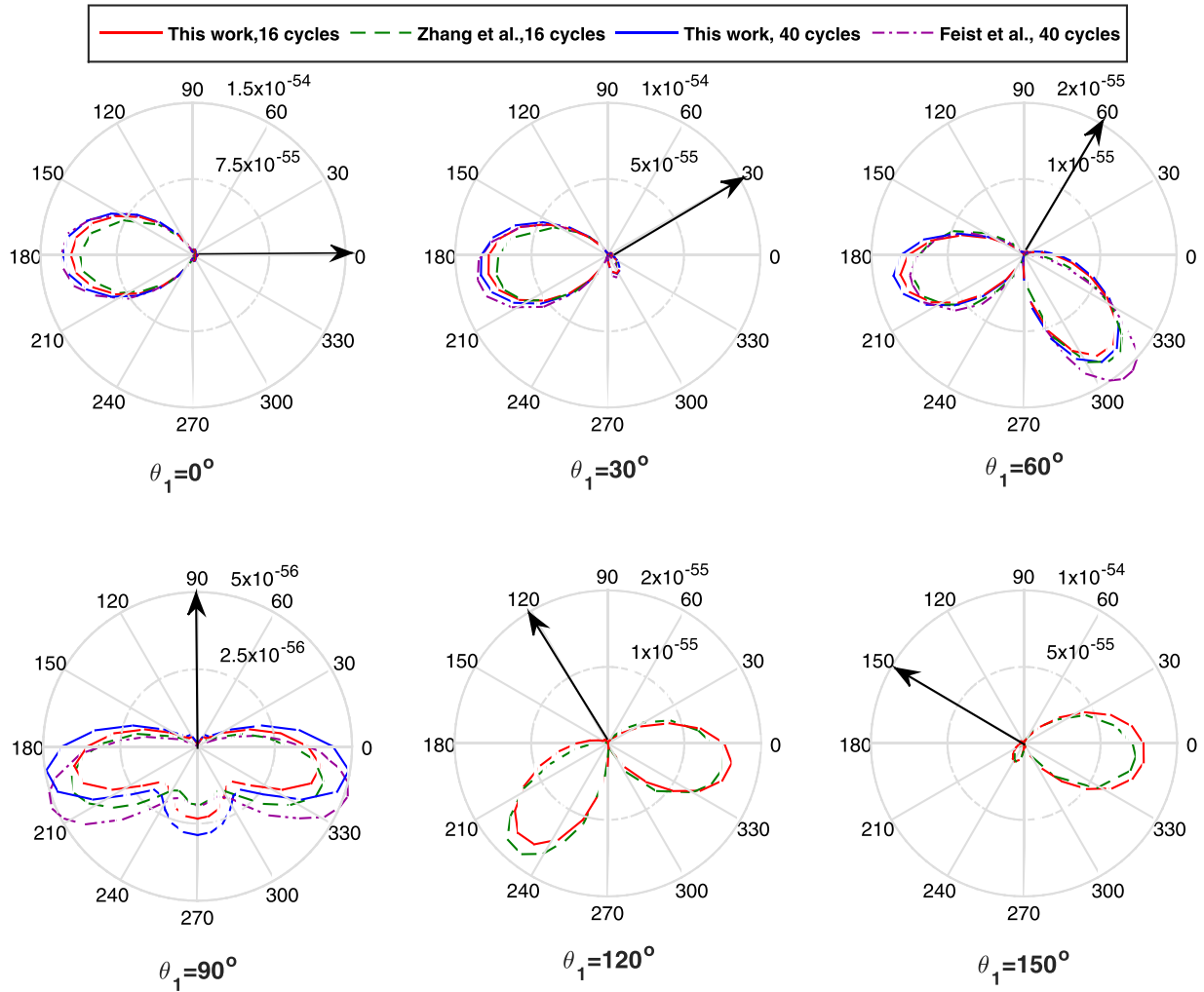


FIG. 3. Polar plots of the TDCS at 42 eV photon energy, for 16 and 40 optical cycles. The TDCS is given as a function of  $\theta_2$ , the angle of one of the ejected electrons. Six values of  $\theta_1$ , the angle of the other ejected electrons, are considered:  $0^\circ$ ,  $30^\circ$ ,  $60^\circ$ ,  $90^\circ$ ,  $120^\circ$ , and  $150^\circ$ . The results for the present work (red solid line for 16 cycles and blue solid line for 40 cycles) are compared with those obtained by Zhang *et al.* [10] (green dashed line) and Feist *et al.* [16] (purple dash-dotted line).

projected on the convergent close-coupling correlated final state, while CCC closure refers to the convergent close-coupling correlated final state using closure approximation.

Observing these plots, we notice minima, materialized by dips for the angle  $\theta_1 = \theta_2$ , indicating that the two electrons try to avoid escaping in the same direction due to Coulombian repulsion. It was reported in Ref. [35] that these minima (practically zero) appear only in a completely converged calculation. This behavior is the consequence of electron correlation during the interaction of the electrons with the laser pulse. It is clear that the Coulomb repulsive correlation between the two electrons will always force them to depart from each other and not in the same direction. All theoretical approaches presented in Fig. 2 reproduce these minima except the CCC calculations.

Figure 3 shows the polar plots of the TDCS at a photon energy of 42 eV for 16 and 40 optical cycles. The TDCS is given as a function of  $\theta_2$ , the angle of one of the ejected electrons. The present work is compared to those of Zhang *et al.* [10] and Feist *et al.* [16]. Zhang *et al.* employed spherical coordinates and the close-coupling scheme to treat the

angular coordinates analytically. The final state was made by projection of the wave function onto the product of two Coulomb waves after propagating for a long time until reaching the supposed asymptotic region. Feist *et al.* employed time-dependent *ab initio* calculations with the wave function projected onto uncorrelated final states at the end of the field interaction.

For the two numbers of optical cycles considered, the present results are close to all the results of Zhang *et al.* and those of Feist *et al.* (see also Fig. 2) including the reported most unfavored emission direction case  $\theta_1 = 90^\circ$ . However, for this reported most challenging case, a little shift is observed and our result also shows a little more pronounced peak at  $\theta_2 \simeq 270^\circ$ . This suggests that at this angle, back-to-back ejection might be more likely. For  $\theta_1 = 60^\circ$ , the result of Feist *et al.* for 40 cycles slightly overestimates ours at  $\theta_2 \simeq 310^\circ$ . Overall, the agreement between the approaches is between a factor of 1.1 and 1.2.

With an arrow indicating on these polar representations the fixed ejection axis of electron 1 relative to the direction of polarization, we better see that the two electrons are mainly

ejected along the laser polarization axis. This is more clearly demonstrated in the cases where TDCSs have only one lobe as  $\theta_1 = 0^\circ$ . For other angles of  $\theta_1$  such as  $\theta_1 = 60^\circ$  and  $120^\circ$  there are two peaks appearing at specific  $\theta_2$  angles. Hu *et al.* [21], after analysis, attributed dips in this particular case to destructive interference between the  $L = 0$  and  $L = 2$  components.

#### IV. CONCLUSION

In this paper we have proposed a nonpropagate wave function based on a correlated Coulomb-Volkov approach to solve the TDSE of an atomic two-electron system. We applied it to the angular distributions of the nonsequential two-photon double ionization of helium. The total two-photon double-ionization cross section was presented for photon energies ranging from 39.5 to 54 eV and also the triple-differential cross sections at a photon energy of 42 eV.

Concerning the results obtained, we found good agreement when comparing our results for the total two-photon double-ionization cross section with the results obtained in previous calculations, in which the cross sections were extracted by projecting the time-propagated wave function onto the uncorrelated product of Coulomb functions [13,16,20,21,31]. Fairly good agreement was also found with approaches including correlation in the final states [18,32], except for the result presented in [13]. The same trend was observed with the results of the triple-differential cross section for two-photon double ionization where our result is closer in shape and in magnitude to those in Refs. [10,11,16] than (in shape) to those in Ref. [19].

In this work we used a correlated wave function to describe the continuum states and in the end we found good agreement with approaches using projections onto uncorrelated continuum states. The comparative assessment carried out showed that the disagreements that remain between some theoretical models for the process studied cannot simply be attributed to the role of electronic correlation in the continuum states. As reported in [34], one of the sources of disagreements encountered by some theoretical models has a highly probable cause in the reflection of the ionized wave packet and precisely of the fast electrons coming from the first channels of single ionization, at the artificial boundaries imposed by the basis functions. The subject remains open and experimental results are welcome. We are of the opinion that the proposed approach in this work, which does not require propagation of the wave packet, could be applied to several other ionization processes involving XUV laser pulses.

#### ACKNOWLEDGMENTS

The authors are grateful to the Abdus Salam International Center for Theoretical Physics (ICTP) for its support through the OEA-AF-12 project. The Centre for Atomic Molecular Physics and Quantum Optics (CEPAMOQ) of the University of Douala (Cameroon) is the ICTP affiliated Centre in Central Africa. The authors wish to thank Prof. Yu. V. Popov and Prof. B. Piraux for interesting discussions about many aspects of Sturmian functions and three-body Coulomb problems.

#### APPENDIX: TEMPORAL PART OF THE TRANSITION AMPLITUDE

According to (24) for the temporal part of the transition amplitude, the time integration over the pulse duration is of the form

$$Q_{k_1 k_2}(t) = \int_0^\tau dt A(t) E(t) \exp\left(i(\varepsilon_{k_1} + \varepsilon_{k_2} - \varepsilon_{H_e})t + (\mathbf{k}_1 + \mathbf{k}_2) \int_\tau^t dt' A(t')\right). \quad (\text{A1})$$

According to [28],  $(\mathbf{k}_1 + \mathbf{k}_2) \int_\tau^t dt' A(t')$  is considered as a correction and can be neglected compared to the term to its left. Therefore, Eq. (A1) becomes

$$Q_{k_1 k_2}(t) = \int_0^\tau dt A(t) E(t) \exp[i(\varepsilon_{k_1} + \varepsilon_{k_2} - \varepsilon_{H_e})t]. \quad (\text{A2})$$

Knowing that  $A(t) = -\int_0^\tau dt' E(t')$  and using (4), we can write

$$E(t) = E_0 \left[ \sin(\omega t + \varphi) \left( \frac{1 - \cos\left(\frac{2\pi t}{\tau}\right)}{2} \right) \right] = -\frac{E_0}{4} \left\{ \sin \left[ \left( \omega + \frac{2\pi}{\tau} \right) t + \varphi \right] + \sin \left[ \left( \omega - \frac{2\pi}{\tau} \right) t + \varphi \right] \right\} + \frac{E_0}{2} \sin(\omega t + \varphi)$$

and

$$A(t) = B + C \cos(\omega t + \varphi) + D \cos(\omega_p t + \varphi) + H \cos(\omega_m t + \varphi),$$

where

$$B = \frac{\left(\frac{2\pi}{\tau}\right)^2 E_0}{2\omega(\omega_p \omega_m)} \cos \varphi, \quad C = \frac{E_0}{2\omega}, \quad D = -\frac{E_0}{4\omega_p}, \quad H = -\frac{E_0}{4\omega_m},$$

with  $\omega_p = \omega + \frac{2\pi}{\tau}$  and  $\omega_m = \omega - \frac{2\pi}{\tau}$ .



By writing  $\alpha = \varepsilon_{k_1} + \varepsilon_{k_2} - \varepsilon_{H_c}$ ,  $Q_{k_1 k_2}(t)$  becomes

$$\begin{aligned} Q_{k_1 k_2}(t) &= B \int_0^\tau dt E(t) \exp(i\alpha t) + C \int_0^\tau dt E(t) \exp(i\alpha t) \cos(\omega t + \varphi) \\ &\quad + D \int_0^\tau dt E(t) \exp(i\alpha t) \cos(\omega_p t + \varphi) + H \int_0^\tau dt E(t) \exp(i\alpha t) \cos(\omega_m t + \varphi) \\ &= Q_1(t) + Q_2(t) + Q_3(t) + Q_4(t). \end{aligned} \quad (\text{A3})$$

Equation (A3) is a sum of four integrals that can be easily solved. For example, let us take the second integral and write it as

$$Q_2(t) = C \int_0^\tau dt E(t) \exp(i\alpha t) \cos(\omega t + \varphi). \quad (\text{A4})$$

By using the exponential form of the cosine function,  $Q_2(t)$  becomes

$$\begin{aligned} Q_2(t) &= C \left( \frac{\exp(i\varphi)}{2} \int_0^\tau dt E(t) \exp[i(\alpha + \omega)t] + \frac{\exp(-i\varphi)}{2} \int_0^\tau dt E(t) \exp[i(\alpha - \omega)t] \right) \\ &= C \left( v \int_0^\tau dt E(t) \exp(i\varepsilon_2 t) + s \int_0^\tau dt E(t) \exp(i\varepsilon_3 t) \right), \end{aligned} \quad (\text{A5})$$

where  $\varepsilon_2 = \alpha + \omega$ ,  $\varepsilon_3 = \alpha - \omega$ ,  $v = \frac{\exp(i\varphi)}{2}$ , and  $s = \frac{\exp(-i\varphi)}{2}$ . In (A5)

$$\begin{aligned} \int_0^\tau dt E(t) \exp(i\varepsilon_2 t) &= C_1 \left( \frac{e^{i\mu_1 t}}{\mu_1} + \frac{e^{i\mu_3 t}}{\mu_3} - 2 \frac{e^{i\mu_5 t}}{\mu_5} \right) + \mathcal{D}_1 \left( -\frac{e^{i\mu_2 t}}{\mu_2} + \frac{e^{-i\mu_4 t}}{\mu_4} + 2 \frac{e^{i\mu_6 t}}{\mu_6} \right) + \mathcal{G}_2, \\ \int_0^\tau dt E(t) \exp(i\varepsilon_3 t) &= C_1 \left( \frac{e^{i\rho_1 t}}{\rho_1} + \frac{e^{i\rho_3 t}}{\rho_3} - 2 \frac{e^{i\rho_5 t}}{\rho_5} \right) + \mathcal{D}_1 \left( -\frac{e^{i\rho_2 t}}{\rho_2} + \frac{e^{-i\rho_4 t}}{\rho_4} + 2 \frac{e^{i\rho_6 t}}{\rho_6} \right) + \mathcal{G}_3, \end{aligned}$$

where  $\mathcal{G}_2 = C_1(-\frac{1}{\mu_1} - \frac{1}{\mu_3} + \frac{2}{\mu_5}) + \mathcal{D}_1(\frac{1}{\mu_2} - \frac{1}{\mu_4} - \frac{2}{\mu_6})$ ,  $\mathcal{G}_3 = C_1(-\frac{1}{\rho_1} - \frac{1}{\rho_3} + \frac{2}{\rho_5}) + \mathcal{D}_1(\frac{1}{\rho_2} - \frac{1}{\rho_4} - \frac{2}{\rho_6})$ ,  $C_1 = \frac{1}{8}[E_0 \cos \varphi + iE_0 \sin(\varphi)]$ ,  $\mathcal{D}_1 = \frac{1}{8}[E_0 \cos \varphi - iE_0 \sin(\varphi)]$ ,  $\mu_6 = \varepsilon_2 - \omega$ ,  $\mu_5 = \varepsilon_2 + \omega$ ,  $\mu_4 = 2\beta - \mu_6$ ,  $\mu_3 = -2\beta - \mu_5$ ,  $\mu_2 = 2\beta + \mu_6$ ,  $\mu_1 = 2\beta + \mu_5$ ,  $\rho_6 = \varepsilon_3 - \omega$ ,  $\rho_5 = \varepsilon_3 + \omega$ ,  $\rho_4 = 2\beta - \rho_6$ ,  $\rho_3 = -2\beta - \rho_5$ ,  $\rho_2 = 2\beta + \rho_6$ , and  $\rho_1 = 2\beta + \rho_5$ , with  $\beta = \pi/\tau$ . By substituting all these expressions in (A5),  $Q_2(t)$  can finally be written as

$$\begin{aligned} Q_2(t) &= C \left\{ v \left[ C_1 \left( \frac{e^{i\mu_1 t}}{\mu_1} + \frac{e^{i\mu_3 t}}{\mu_3} - 2 \frac{e^{i\mu_5 t}}{\mu_5} \right) + \mathcal{D}_1 \left( -\frac{e^{i\mu_2 t}}{\mu_2} + \frac{e^{-i\mu_4 t}}{\mu_4} + 2 \frac{e^{i\mu_6 t}}{\mu_6} \right) + \mathcal{G}_2 \right] \right. \\ &\quad \left. + s \left[ C_1 \left( \frac{e^{i\rho_1 t}}{\rho_1} + \frac{e^{i\rho_3 t}}{\rho_3} - 2 \frac{e^{i\rho_5 t}}{\rho_5} \right) + \mathcal{D}_1 \left( -\frac{e^{i\rho_2 t}}{\rho_2} + \frac{e^{-i\rho_4 t}}{\rho_4} + 2 \frac{e^{i\rho_6 t}}{\rho_6} \right) + \mathcal{G}_3 \right] \right\}. \end{aligned} \quad (\text{A6})$$

- 
- [1] E. A. Hylleraas and J. Midtdal, *Phys. Rev.* **103**, 829 (1956).  
[2] E. A. Hylleraas and J. Midtdal, *Phys. Rev.* **109**, 1013 (1958).  
[3] T. Kinoshita, *Phys. Rev.* **105**, 1490 (1957).  
[4] C. L. Pekeris, *Phys. Rev.* **112**, 1649 (1958).  
[5] J. N. Silverman, O. Platas, and F. A. Matsen, *J. Chem. Phys.* **32**, 1402 (1960).  
[6] C. Schwartz, *Phys. Rev.* **128**, 1146 (1962).  
[7] A. S. Kheifets and I. Bray, *Phys. Rev. A* **58**, 4501 (1998).  
[8] A. S. Kheifets and I. Bray, *Phys. Rev. Lett.* **81**, 4588 (1998).  
[9] A. S. Kheifets and I. Bray, *J. Phys. B* **31**, L447 (1998).  
[10] Z. Zhang, L.-Y. Peng, M.-H. Xu, A. F. Starace, T. Morishita, and Q. Gong, *Phys. Rev. A* **84**, 043409 (2011).  
[11] A. Simonsen, S. Askeland, and M. Førre, *Cent. Eur. J. Phys.* **11**, 1099 (2013).  
[12] F. Reynal, Ph.D. thesis, Université Bordeaux 1, 2012.  
[13] E. Fomouuo, P. Antoine, B. Piraux, L. Malegat, H. Bachau, and R. Shakeshaft, *J. Phys. B* **41**, 051001 (2008); B. Piraux, E. Fomouuo, P. Antoine, and H. Bachau, *J. Phys.: Conf. Ser.* **141**, 012013 (2008).  
[14] H. Hasegawa, E. J. Takahashi, Y. Nabekawa, K. L. Ishikawa, and K. Midorikawa, *Phys. Rev. A* **71**, 023407 (2005).  
[15] A. A. Sorokin, M. Wellhöfer, S. V. Bobashev, K. Tiedtke, and M. Richter, *Phys. Rev. A* **75**, 051402(R) (2007).  
[16] J. Feist, S. Nagele, R. Pazourek, E. Persson, B. I. Schneider, L. A. Collins, and J. Burgdörfer, *Phys. Rev. A* **77**, 043420(R) (2008).  
[17] A. S. Kheifets and I. A. Ivanov, *J. Phys. B* **39**, 1731 (2006).  
[18] A. S. Kheifets, I. A. Ivanov, and I. Bray, *J. Phys.: Conf. Ser.* **88**, 012051 (2007).  
[19] I. A. Ivanov and A. S. Kheifets, *Phys. Rev. A* **75**, 033411 (2007).  
[20] X. Guan, O. Zatsarinny, C. J. Noble, K. Bartschat, and B. I. Schneider, *J. Phys. B* **42**, 134015 (2009); X. Guan, K. Bartschat, and B. I. Schneider, *Phys. Rev. A* **77**, 043421 (2008).  
[21] S. X. Hu, J. Colgan, and L. A. Collins, *J. Phys. B* **38**, L35 (2005).  
[22] G. Duchateau, Ph.D. thesis, Université Bordeaux 1, 2001.

- [23] M. S. Mengoue, M. G. K. Njock, B. Piraux, Y. V. Popov, and S. A. Zaytsev, *Phys. Rev. A* **83**, 052708 (2011); S. M. Marius, Ph.D. thesis, Université de Douala, 2012.
- [24] E. Fomouuo, G. L. Kamta, G. Edah, and B. Piraux, *Phys. Rev. A* **74**, 063409 (2006).
- [25] F. H. M. Faisal, *Phys. Rev. A* **94**, 031401(R) (2016).
- [26] J. Vâbek, H. Bachau, and F. Catoire, *Phys. Rev. A* **106**, 053115 (2022).
- [27] K. Amini, J. Biegert, F. Calegari, A. Chacón, M. F. Ciappina, A. Dauphin, D. K. Efimov, C. F. de Morisson Faria, K. Giergiel, P. Gniewek *et al.*, *Rep. Prog. Phys.* **82**, 116001 (2019).
- [28] R. Guichard, H. Bachau, E. Cormier, R. Gayet, and V. D. Rodriguez, *Phys. Scr.* **76**, 397 (2007).
- [29] M. Silenou Mengoue, *Phys. Rev. A* **87**, 022701 (2013).
- [30] G. W. F. Drake, *Phys. Rev. Lett.* **65**, 2769 (1990).
- [31] S. Laulan and H. Bachau, *Phys. Rev. A* **68**, 013409 (2003).
- [32] L. Feng and H. W. van der Hart, *J. Phys. B* **36**, L1 (2003).
- [33] I. Ivanov and A. Kheifets, *J. Phys. B* **41**, 095002 (2008).
- [34] A. Hamido, Ph.D. thesis, Université Catholique de Louvain, 2014; L. Malegat, H. Bachau, A. Hamido, and B. Piraux, *J. Phys. B* **43**, 245601 (2010).
- [35] D. A. Horner, C. W. McCurdy, and T. N. Rescigno, *Phys. Rev. A* **78**, 043416 (2008).